Suppression of excited-state absorption: A path to ultraviolet tunable solid-state lasers

Elena Kuznetsova,* Roman Kolesov, and Olga Kocharovskaya
Department of Physics, Texas A&M University, College Station, Texas 77843-4242, USA
and Institute of Applied Physics RAS, 46 Ulyanov Street, Nizhny Novgorod 603950, Russia
(Received 16 January 2004; published 4 October 2004)

A method of suppression of losses due to excited-state absorption (ESA) in laser crystals is proposed, based on the well-known phenomenon of electromagnetically induced transparency. Typical situations in which ESA prevents lasing are considered. Theoretical analysis shows that by using an additional driving laser field one can inhibit ESA and make lasing possible. On the basis of available spectroscopic information estimates for rare-earth-ion-doped laser materials are presented. They show the feasibility of obtaining optical gain at parity-allowed $4f^n \leftrightarrow 4f^{n-1}5d$ transitions of rare-earth ions in the ultraviolet spectral region after suppression of ESA at an emission wavelength into the conduction band of a host material.

DOI: 10.1103/PhysRevA.70.043801 PACS number(s): 42.55.Rz, 42.50.Gy, 42.70.Hj

I. INTRODUCTION

Currently, a lot of experimental effort in solid-state optics is devoted to searching for laser materials suitable for tunable lasing, primarily in the uv and vacuum uv (vuv) spectral regions. Mainly, researchers focus on optical crystals doped with either transition metal or rare-earth ions [1]. The latter doped into wide band gap dielectric crystals have spectrally broad vibronic emission bands associated with $4f^{n-1}5d \leftrightarrow 4f^n$ interconfigurational transitions, whose energies lie mostly in the uv or vuv regions of the spectrum. The transitions are electric dipole allowed; therefore they have large absorption and emission cross sections, and are promising for efficient tunable laser action. Interest in impurity-doped crystals is also motivated by the fact that similar lasing media in the visible and near infrared are very robust and easy to operate. The most famous examples are Ti:sapphire, Nd:YAG (yttrium aluminum garnet), Nd:YLF, and Yb:YAG systems which can deliver high laser power in both continuous wave and pulsed regimes.

However, not much progress has been made in developing solid-state uv and vuv lasers. Thus far laser action in the uv was realized in several Ce^{3+}-doped dielectric host materials, emitting wavelengths tunable in the range 270–310 nm [2]; in the vuv region only $Nd^{3+}:LaF_3$ demonstrates lasing with exceptionally large photon energy corresponding to 172 nm wavelength with the possibility of tuning from 170 nm to 175 nm [3]. Most of the materials in which laser oscillation has been observed are listed in [1,4].

There are two major obstacles in the way of making an impurity-doped crystal lase in the uv or vuv. First of all, one has to create population inversion at an operating transition, which requires very high pump power densities, scaling as ν^3 with the frequency of the pump. This problem can be rather satisfactorily solved by introducing two- or three-step pumping via intermediate states of a dopant ion with visible or near-uv light (see, for example, [5]). It also helps to prevent formation of color center defects, produced by strong uv pumping and causing additional optical losses. The second problem is more fundamental. It is the so-called excited-state absorption (ESA), i.e., absorption from metastable laser levels to higher-energy states. The terminal state for ESA can be either a higher-lying discrete level or the conduction band (CB) of a crystal. In the majority of rare-earth-ion-doped materials ESA at emission or/and pump wavelengths reduces the efficiency or completely prohibits laser action. This happens if the ESA cross section σ_{ESA} exceeds the stimulated-emission cross section σ_{SE}. For $Nd^{3+}:LaF_3$ and Ce^{3+}-doped materials lasing is possible because, luckily, $\sigma_{SE} > \sigma_{ESA}$. Moreover, in many cases ESA prevents lasing not only in the uv and vuv parts of the spectrum, but also in the visible and in the infrared. Some (but not the only) examples of the materials in which laser action cannot be observed due to ESA are the following: $Ce^{3+}:YAG$ [7] (red to green luminescence), $Yb^{2+}:CaF_2$ [4] (red to blue luminescence), $Yb^{2+}:MgF_2$ [8] (blue luminescence), $Eu^{2+}:CaF_2$ [10] (blue luminescence), $Pr^{3+}:YAG$ [6] (blue to near uv luminescence), $Pr^{3+}:YLF$ [9] (uv luminescence), $Nd^{3+}:YLF$ [11] (vuv luminescence), and many others.

In the present paper a method for reduction of excited-state absorption is proposed, which makes use of the well-known phenomenon of electromagnetically induced transparency (EIT) [12]; namely, absorption from a populated excited electronic state can be suppressed under the action of an additional driving coherent field, resonantly coupling the terminal state of ESA to some intermediate discrete state. In this work we study the possibility to suppress ESA at a desired wavelength of laser oscillation in rare-earth-ion-doped laser materials.

The outline of the paper is as follows. In Sec. II the most common level configurations in which ESA can occur are reviewed, and a simplified model of ESA suppression is developed. In Sec. III estimates for the efficiency of ESA reduction and required intensities of the driving field are presented for typical parameters of dielectric host materials doped with rare-earth ions. Finally, we consider in more detail a particular material $Pr^{3+}:LiLuF_4$ in which uv laser action can be realized using the proposed method.

*Corresponding author. Email address: lena@jewel.tamu.eduF

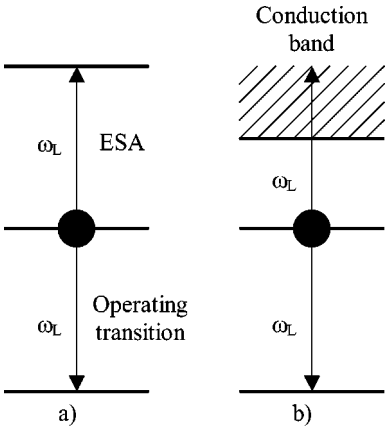

FIG. 1. ESA at the laser oscillation wavelength in crystals activated with rare-earth ions.

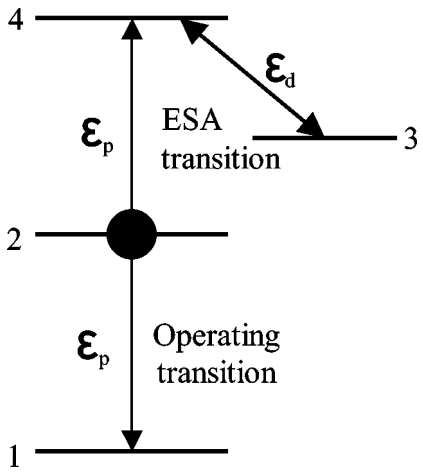

FIG. 2. ESA to discrete terminal level.

II. TYPICAL ESA CONFIGURATIONS

We start by reviewing common configurations in which ESA can prevent laser action. We focus on ESA reduction in wide band gap optical crystals doped with divalent or trivalent rare-earth ions because these materials are considered to be the most promising for uv and vuv solid-state lasing.

Typically, rare-earth ions enter crystals in a trivalent state, but some of them (Ce, Pr, Eu, Yb, Tm, and Sm) can be stabilized in a divalent state. In both cases the ground state of a rare-earth ion is $4f^n$ with Ce^{2+} being the only exception [13]. Energies of excited $4f^n$ levels typically extend from the ir into the vuv region while energies of $4f^{n-1}5d$ levels mostly lie in the uv and vuv parts of the spectrum. Parity-forbidden $4f^n \leftrightarrow 4f^n$ transitions are rather weak (typical absorption and stimulated-emission cross sections are $\sigma \sim 10^{-21}-10^{-20}$ cm^2) compared to the much stronger parity-allowed $4f^n \leftrightarrow 4f^{n-1}5d$ transitions ($\sigma \sim 10^{-19}-10^{-18}$ cm^2). Having at the same time broad emission and absorption bands, these interconfigurational transitions offer the potential for wavelength-tunable laser operation. $4f^n \leftrightarrow 4f^n$ transitions can be used for laser operation at a fixed wavelength in the uv or vuv.

The terminal level for ESA can be either a higher-lying discrete state [Fig. 1(a)] or continuum states in the CB [Fig. 1(b)]. In the next subsections we will analyze these two configurations separately and derive conditions for ESA suppression due to EIT. ESA can also originate from charge transfer processes, but we do not consider this situation in the present paper.

A. Discrete terminal level for ESA

Consider the situation, depicted in Fig. 1(a), in which ESA occurs from an upper operating state of a laser transition to a higher-lying discrete state. By resonantly coupling the terminal state 4 of the ESA transition to some auxiliary state 3 by an additional driving field, one can suppress absorption of the emitted field, as is depicted in Fig. 2.

It is worth mentioning that in Refs. [14] the idea of using an additional control field in order to manipulate absorption properties of a medium was applied to inhibit two-photon absorption (TPA). TPA from a ground state to some excited state as well as stepwise excitation were suppressed by using the control field, coupling an intermediate state via which TPA occurred to some auxiliary state. In the system which we consider it is absorption from the excited, not the ground, state that is to be suppressed; therefore the additional driving field has to couple the auxiliary state to the terminal rather than to the initial state of the ESA transition. In the case of a discrete terminal level, as in Fig. 2, the additional state 3 can be either of lower or higher energy with respect to the terminal state 4, so that the ESA transition $2 \leftrightarrow 4$ and the adjacent transition $3 \leftrightarrow 4$ can form either Λ- type or ladder systems, provided that the coherence at the two-photon transition $2 \leftrightarrow 3$ is sufficiently long lived.

In order to derive conditions at which laser oscillation can be achieved, we consider linear gain/loss for a weak probe field ε_p in an active medium. To that end we calculate the total optical polarization of the medium due to the probe field resonant with transitions $2 \leftrightarrow 1$ and $4 \leftrightarrow 2$. The ultimate goal is to obtain conditions under which the probe field is amplified in the presence of the driving field while in the absence of one it is absorbed.

Density matrix equations describing medium polarization in a linear approximation with respect to the probe field can be written in the following form:

$$\dot{\sigma}_{42} + i(\omega_{42} - \omega_p)\sigma_{42} + i\frac{\varepsilon_p \mu_{42}}{2\hbar}(\rho_{44} - \rho_{22}) - i\frac{\varepsilon_d \mu_{43}}{2\hbar}\sigma_{32} = -\gamma_{42}\sigma_{42}, \quad (1)$$

$$\dot{\sigma}_{21} + i(\omega_{21} - \omega_p)\sigma_{21} + i\frac{\varepsilon_p \mu_{21}}{2\hbar}(\rho_{22} - \rho_{11}) = -\gamma_{21}\sigma_{21}, \quad (2)$$

$$\dot{\sigma}_{32} + i(\omega_{32} + \omega_d - \omega_p)\sigma_{32} - i\frac{\varepsilon_d^* \mu_{43}^*}{2\hbar}\sigma_{42} + i\frac{\varepsilon_p \mu_{42}}{2\hbar}\sigma_{43}^* = -\gamma_{32}\sigma_{32}, \quad (3)$$

$$\dot{\sigma}_{43} + i(\omega_{43} - \omega_d)\sigma_{43} + i\frac{\varepsilon_d \mu_{43}}{2\hbar}(\rho_{44} - \rho_{33}) - i\frac{\varepsilon_p \mu_{42}}{2\hbar}\sigma_{32}^{*} = -\gamma_{43}\sigma_{43}. \tag{4}$$

Here ω_p and ω_d are the frequencies of the probe and driving fields, respectively, μ_{mn} is the dipole moment of the $m \leftrightarrow n$ transition, σ_{mn} are the complex amplitudes of the off-diagonal density matrix elements in the rotating-wave approximation (RWA), and γ_{mn} are their corresponding decay rates.

A steady-state solution of the above set of equations yields the following result for the complex amplitude of a net polarization of the medium at the probe field frequency:

$$P = N(\sigma_{21}\mu_{12} + \sigma_{42}\mu_{24}) = i\frac{\varepsilon_p N}{2\hbar}\left(\frac{|\mu_{21}|^2(\rho_{11} - \rho_{22})}{i(\omega_{21} - \omega_p) + \gamma_{21}} + \frac{|\mu_{42}|^2\left(\rho_{22} - \rho_{44} + \left|\frac{\varepsilon_d \mu_{43}}{2\hbar}\right|^2 \frac{\rho_{33} - \rho_{44}}{[i(\omega_{43} - \omega_d) - \gamma_{43}][i(\omega_{32} - \omega_p + \omega_d) + \gamma_{32}]}\right)}{i(\omega_{42} - \omega_p) + \gamma_{42} + \left|\frac{\varepsilon_d \mu_{43}}{2\hbar}\right|^2 \frac{1}{i(\omega_{32} - \omega_p + \omega_d) + \gamma_{32}}}\right), \tag{5}$$

where we neglect inhomogeneous broadening. The negative or positive sign of the imaginary part of Eq. (5) determines whether the probe field is amplified or absorbed, respectively, in the medium. We are interested in the case of exact resonance of the probe field with the inverted transition $2 \leftrightarrow 1$ ($\omega_p = \omega_{21}$) and exact resonance of the driving and probe fields with the two-photon transition $3 \leftrightarrow 2$ ($\omega_p - \omega_d = \omega_{32}$). Let us assume also that initially only state 2 is populated. Then, the imaginary part of the polarization takes the form

$$\mathrm{Im}(P) = -\frac{\varepsilon_p N}{2\hbar}\left(\frac{|\mu_{21}|^2(\rho_{22} - \rho_{11})}{\gamma_{21}} - \rho_{22}\frac{|\mu_{42}|^2(\gamma_{42} + |\Omega_d|^2/\gamma_{32})}{(\omega_{42} - \omega_p)^2 + (\gamma_{42} + |\Omega_d|^2/\gamma_{32})^2}\right), \tag{6}$$

where $\Omega_d = \varepsilon_d \mu_{43}/2\hbar$ is the Rabi frequency of the driving field.

All terms in Eq. (6) have clear physical meaning. The first one describes amplification of the probe field in the presence of inversion at the laser transition $2 \leftrightarrow 1$ while the second one describes ESA, modified by the driving field. If $\Omega_d = 0$ (no driving field) and $\rho_{22} = 1$, the imaginary part of the polarization reads

$$\mathrm{Im}(P) = -\frac{\varepsilon_p N}{2\hbar}\left(\frac{|\mu_{21}|^2}{\gamma_{21}} - \frac{|\mu_{42}|^2 \gamma_{42}}{(\omega_{42} - \omega_p)^2 + \gamma_{42}^2}\right). \tag{7}$$

A positive sign of this expression means that $\sigma_{ESA} > \sigma_{SE}$ and no gain for the probe field is possible in the medium. However, for rather strong driving field ($|\Omega_d|^2 > |\Omega_{th}|^2 = \gamma_{32}\gamma_{42}$) ESA can be suppressed by a factor of $|\Omega_d|^2/\gamma_{32}\gamma_{42}$ in the center of the ESA line. Note that the threshold Rabi frequency Ω_{th} of the driving field corresponds to the standard EIT threshold [12]. This is expected since transitions $2 \leftrightarrow 4$ and $3 \leftrightarrow 4$ form a Λ system, in which one-photon absorption from state 2 is suppressed due to EIT if a strong driving field is applied to the adjacent transition. In order to achieve gain the driving field Rabi frequency has to match the condition

$$|\Omega_d|^2 > |\Omega_0|^2 = \frac{\sigma_{ESA}}{\sigma_{SE}}\Omega_{th}. \tag{8}$$

In the above analysis inhomogeneous broadening was not taken into account. In a solid medium the standard EIT threshold Rabi frequency in a Λ system is modified. As is shown in Ref. [15], in the case of rare-earth-ion-doped crystals the modification is that inhomogeneous linewidths of transitions have to be substituted instead of homogeneous ones, so that $|\Omega_{th}|^2 = W_{42}^{inh} W_{32}^{inh}$.

B. ESA into the conduction band

In this subsection we show that ESA terminating in the CB of a host material can be reduced in a similar way as in the case of a discrete terminal level. The phenomenon of inhibited photoionization has been known since 1961 when Fano theoretically explained experimental data on photoionization reduction in helium arising from interaction of a discrete autoionizing state, embedded into the continuum, with continuum states [16]. The origin of the reduction is the destructive interference of probability amplitudes of two pathways leading to ionization. Later, it was discovered that a Fano-type continuum structure can be realized in a structureless continuum by admixing a bound electronic state into the continuum with a laser [17]. This phenomenon is called laser-induced continuum structure (LICS) and it is very well studied in rare gases (for recent experimental results, see, for example, [18] and references therein).

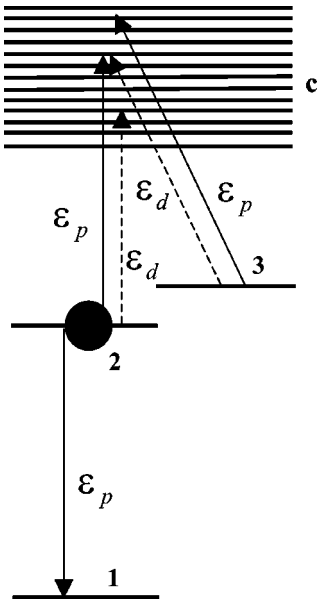

FIG. 3. ESA to continuum terminal levels.

In order to show that ESA into the CB can be reduced in the same manner as in the previous subsection, we consider a simple four-level model system, depicted in Fig. 3, in which the state 4 is now replaced by continuum electronic states in the CB. We treat it as a structureless nondegenerate one-dimensional continuum, which means that each electronic energy state in the CB is described by only one quantum number—its energy. This assumption will make our consideration much simpler and reveal the essential physics of the problem. In reality, however, more than one continuum can be involved in the ESA process. For example, in the case of ESA originating from a $4f^{n-1}5d$ level, the terminal state of an electron in the CB can be either *p*-like or *f*-like.

The following assumptions are used in the analysis: (1) the medium is prepared in state 2, so that no other state is populated; (2) both probe and driving fields couple corresponding discrete levels to the same continuum; (3) fields are resonant only with transitions designated in Fig. 3; (4) wave-mixing processes are neglected; (5) only the linear response of the medium to the probe field is analyzed in order to calculate the linear gain.

The wave function describing this three-level + continuum system is

$$|\Psi\rangle = A_1|1\rangle + A_2|2\rangle + A_3|3\rangle + \int C|c\rangle dE_c.$$

The Hamiltonian of the system is $\hat{H}=\hat{H}_0+\hat{V}$, where the nonperturbed and perturbation Hamiltonians are given by the expressions

$$\hat{H}_0 = E_1|1\rangle\langle 1| + E_2|2\rangle\langle 2| + E_3|3\rangle\langle 3| + \int E_c|c\rangle\langle c|dE_c,$$

$$\hat{V} = -\mu_{21}\varepsilon|2\rangle\langle 1| - \int \mu_{c2}\varepsilon|c\rangle\langle 2|dE_c - \int \mu_{c3}\varepsilon|c\rangle\langle 3|dE_c + \text{c.c.},$$

and two laser fields are applied:

$$\varepsilon = \sum_j \frac{\varepsilon_j}{2} e^{-i\omega_j t + ik_j z} + \text{c.c.}, \quad j = p,d.$$

As in the previous subsection ε_p is the probe field, which is absorbed from the emitting level 2 into the continuum and amplified at the $2\leftrightarrow 1$ transition; ε_d is the driving field, applied at the adjacent $3\leftrightarrow c$ transition, which inhibits ESA of the probe field if certain conditions are met, as will be shown below. Both fields are assumed to be plane waves propagating in the *z* direction.

Using the interaction representation for complex amplitudes of quantum states $a_n=A_n e^{iE_n t/\hbar}$, $c=Ce^{iE_c t/\hbar}$ as well as the RWA, and adiabatically eliminating the continuum following the procedure of Ref. [17], we effectively reduce the system to a three-level one:

$$i\hbar\frac{\partial a_1}{\partial t} = -\frac{\mu_{12}\varepsilon_p^*}{2} a_2 e^{-i[(E_2-E_1)/\hbar-\omega_p]t-ik_p z}, \tag{9}$$

$$\begin{aligned} i\hbar\frac{\partial a_2}{\partial t} = &-\frac{\mu_{21}\varepsilon_p}{2} a_1 e^{i[(E_2-E_1)/\hbar-\omega_p]t+ik_p z} - a_2\left(\frac{|\varepsilon_p|^2}{4\hbar}(P_2^p + i\Gamma_2^p/2)\right. \\ &\left. + \frac{|\varepsilon_d|^2}{4\hbar}(P_2^d + i\Gamma_2^d/2)\right) \\ &- a_3\frac{\varepsilon_p^*\varepsilon_d}{4\hbar} e^{-i[(E_3-E_2)/\hbar-\omega_p+\omega_d]t-i(k_p-k_d)z}(\Pi_{23}^d + iG_{23}^d/2), \end{aligned} \tag{10}$$

$$i\hbar\frac{\partial a_3}{\partial t} = -a_3\left(\frac{|\varepsilon_p|^2}{4\hbar}(P_3^p + i\Gamma_3^p/2) + \frac{|\varepsilon_d|^2}{4\hbar}(P_3^d + i\Gamma_3^d/2)\right) \tag{11}$$

$$- a_2\frac{\varepsilon_p\varepsilon_d^*}{4\hbar} e^{i[(E_3-E_2)/\hbar-\omega_p+\omega_d]t+i(k_p-k_d)z}(\Pi_{32}^p + iG_{32}^p/2).$$

Here we introduce the following notation

$$\begin{aligned} P_m^l + i\Gamma_m^l/2 &= \lim_{\eta\to+0}\int \frac{|\mu_{cm}|^2 dE_c}{(E_c-E_m)/\hbar - \omega_l - i\eta} \\ &= P\int \frac{|\mu_{cm}|^2 dE_c}{(E_c-E_m)/\hbar-\omega_l} + i\pi\hbar|\mu_{cm}|^2_{E_c=E_m+\hbar\omega_l}, \end{aligned} \tag{12}$$

$$\begin{aligned} \Pi_{sq}^l + iG_{sq}^l/2 &= \lim_{\eta\to+0}\int \frac{\mu_{sc}\mu_{cq}dE_c}{(E_c-E_m)/\hbar - \omega_l - i\eta} \\ &= P\int \frac{\mu_{sc}\mu_{cq}dE_c}{(E_c-E_m)/\hbar-\omega_l} + i\pi\hbar\mu_{sc}\mu_{cq|E_c=E_m+\hbar\omega_l}, \end{aligned} \tag{13}$$

with $s,q,m=2$ or 3 and $l=p$ or d. In the above expressions

P_m^l is the dynamic Stark shift of the mth state due to interaction with the lth component of the optical field, Γ_m^l is the ionization rate of the mth level due to the lth field, and Π_{sq}^l and G_{sq}^l together determine the magnitude and the phase of the coherence at the transition $s \leftrightarrow q$ excited due to a Raman process via the continuum.

Let us now turn to the dynamic equations for the amplitudes σ_{ml} of the density matrix $\rho_{ml}=A_m A_l^*$, determined by standard formulas: $\sigma_{21}=\rho_{21}e^{-i\omega_p t+ik_p z}$, $\sigma_{32}=\rho_{32}e^{-i(\omega_p-\omega_d)t+i(k_p-k_d)z}$, $\sigma_{31}=\rho_{31}e^{-i(2\omega_p-\omega_d)t+i(2k_p-k_d)z}$. From Eqs. (9)–(11) one finds

$$\frac{\partial \sigma_{21}}{\partial t} = -\sigma_{21}\Delta_{21} + i\Omega_p(\rho_{11}-\rho_{22}) + i\frac{\varepsilon_p^*\varepsilon_d}{4\hbar^2}\sigma_{31}(\Pi_{23}^d + iG_{23}^d/2), \tag{14}$$

$$\frac{\partial \sigma_{32}}{\partial t} = -\sigma_{32}\Delta_{32} - i\Omega_p^*\sigma_{31} + i\frac{\varepsilon_p\varepsilon_d^*}{4\hbar^2}\{\rho_{22}(\Pi_{32}^p + iG_{32}^p/2) - \rho_{33}[(\Pi_{23}^d)^* - i(G_{23}^d)^*/2]\}, \tag{15}$$

$$\frac{\partial \sigma_{31}}{\partial t} = -\sigma_{31}\Delta_{31} - i\Omega_p\sigma_{32} + i\frac{\varepsilon_p\varepsilon_d^*}{4\hbar^2}\sigma_{21}(\Pi_{32}^p + iG_{32}^p/2), \tag{16}$$

where we use the Rabi frequency of the probe field $\Omega_p=\mu_{21}\varepsilon_p/2\hbar$, and complex dressed decay rates

$$\Delta_{21} = \gamma_{21} + \frac{|\varepsilon_p|^2}{4\hbar^2}\frac{\Gamma_2^p}{2} + \frac{|\varepsilon_d|^2}{4\hbar^2}\frac{\Gamma_2^d}{2} + i\left(\frac{E_2-E_1}{\hbar} - \omega_p - \frac{|\varepsilon_p|^2}{4\hbar^2}P_2^p - \frac{|\varepsilon_d|^2}{4\hbar^2}P_2^d\right),$$

$$\Delta_{32} = \gamma_{32} + \frac{|\varepsilon_p|^2}{4\hbar^2}\frac{\Gamma_2^p+\Gamma_3^p}{2} + \frac{|\varepsilon_d|^2}{4\hbar^2}\frac{\Gamma_2^d+\Gamma_3^d}{2} + i\left(\frac{E_3-E_2}{\hbar} - \omega_p + \omega_d - \frac{|\varepsilon_p|^2}{4\hbar^2}(P_3^p-P_2^p) - \frac{|\varepsilon_d|^2}{4\hbar^2}(P_3^d - P_2^d)\right),$$

$$\Delta_{31} = \gamma_{31} + \frac{|\varepsilon_p|^2}{4\hbar^2}\frac{\Gamma_3^p}{2} + \frac{|\varepsilon_d|^2}{4\hbar^2}\frac{\Gamma_3^d}{2} + i\left(\frac{E_3-E_1}{\hbar} - 2\omega_p + \omega_d - \frac{|\varepsilon_p|^2}{4\hbar^2}P_3^p - \frac{|\varepsilon_d|^2}{4\hbar^2}P_3^d\right),$$

including dynamic Stark shifts, transition broadening due to photoionization, and phenomenological coherence decay rates γ_{ml}. We also introduce the Raman Fano parameters $q^{(1)}=2\Pi_{32}^p/G_{32}^p$ and $q^{(2)}=2\Pi_{23}^d/G_{23}^d$ and assume that both $q^{(1)}$ and $q^{(2)}$ are real. In the vicinity of the two-photon resonance $E_2+\hbar\omega_p=E_3+\hbar\omega_d$, they are approximately equal $q^1\approx q^2\approx q$ because of $\Pi_{32}^p\approx(\Pi_{23}^d)^*$ and $G_{32}^p\approx(G_{23}^d)^*$. Assuming the quasistationarity condition, so that the duration of laser pulses τ satisfies the condition $\tau|\Delta_{21,31,32}|\gg 1$, we neglect time derivatives and obtain coherences that adiabatically follow the fields.

The two-photon coherence reads

$$\sigma_{32} = i\frac{\varepsilon_p\varepsilon_d^*}{4\hbar^2}\frac{G_{32}^p}{2}\frac{|\Omega_p|^2(\rho_{11}-\rho_{22})(q+i) + [\rho_{22}(q+i)-\rho_{33}(q-i)]\left(\Delta_{21}\Delta_{31} + \frac{|\varepsilon_p|^2|\varepsilon_d|^2}{(4\hbar^2)^2}\frac{G_{32}^pG_{23}^d}{4}(q+i)^2\right)}{\Delta_{32}\left(\Delta_{21}\Delta_{31} + \frac{|\varepsilon_p|^2|\varepsilon_d|^2}{(4\hbar^2)^2}\frac{G_{32}^pG_{23}^d}{4}(q+i)^2\right) + \Delta_{21}|\Omega_p|^2}. \tag{17}$$

In the limit of strong driving field ($|\varepsilon_d|^2 \gg |\varepsilon_p|^2$) Eq. (17) reduces to

$$\sigma_{32} = i\frac{\varepsilon_p\varepsilon_d^*}{4\hbar^2}\frac{G_{32}^p}{2}\frac{\rho_{22}(q+i)-\rho_{33}(q-i)}{i\Delta + \frac{|\varepsilon_d|^2}{4\hbar^2}\frac{\Gamma_2^d+\Gamma_3^d}{2} + \gamma_{32}} \tag{18}$$

and

$$\sigma_{21} = \frac{i\Omega_p}{\Delta_{21}}(\rho_{11}-\rho_{22}) = \frac{i\Omega_p(\rho_{11}-\rho_{22})}{iD + \frac{|\varepsilon_d|^2}{4\hbar^2}\frac{\Gamma_2^d}{2} + \gamma_{21}}, \tag{19}$$

where

$$\Delta = \frac{E_3-E_2}{\hbar} - \omega_p + \omega_d - \frac{|\varepsilon_d|^2}{4\hbar^2}(P_3^d - P_2^d),$$

$$D = \frac{E_2-E_1}{\hbar} - \omega_p - \frac{|\varepsilon_d|^2}{4\hbar^2}P_2^d.$$

We can now plug these expressions into the propagation equation for the probe field:

$$\frac{\partial \varepsilon_p}{\partial z} + \frac{n_p}{c}\frac{\partial \varepsilon_p}{\partial t} = \frac{4\pi i\omega_p}{cn_p}P,$$

with polarization of the medium at the probe field frequency given by

$$P = N\left(\sigma_{21}\mu_{12} + \rho_{22}\frac{\varepsilon_p}{2\hbar}(P_2^p + i\Gamma_2^p/2) + \rho_{33}\frac{\varepsilon_p}{2\hbar}(P_3^p + i\Gamma_3^p/2) + \sigma_{32}\frac{\varepsilon_d}{2\hbar}(\Pi_{23}^d + iG_{23}^d/2)\right).$$

Here n_p is the nonresonant refractive index of the medium at the probe frequency.

The population of state 3 is negligible if the driving field is strong (EIT regime), so that the polarization response P reads

$$P = i\frac{\varepsilon_p N}{2\hbar}\left(\frac{|\mu_{21}|^2(\rho_{11}-\rho_{22})}{iD + \frac{|\varepsilon_d|^2}{4\hbar^2}\frac{\Gamma_2^d}{2} + \gamma_{21}} + \rho_{22}(-iP_2^p + \Gamma_2^p/2) + \rho_{22}(q + i)^2\frac{|\varepsilon_d|^2}{4\hbar^2}\frac{G_{32}^p G_{23}^d}{4}\frac{1}{i\Delta + \frac{|\varepsilon_d|^2}{4\hbar^2}\frac{\Gamma_2^d+\Gamma_3^d}{2} + \gamma_{32}}\right).$$

Now we can analyze the imaginary part of the polarization, which determines amplification at the probe wavelength:

$$\mathrm{Im}(P) = -\frac{\varepsilon_p N}{2\hbar}\left[(\rho_{22}-\rho_{11})\frac{|\mu_{12}|^2\left(\frac{|\varepsilon_d|^2}{4\hbar^2}\frac{\Gamma_2^d}{2} + \gamma_{21}\right)}{D^2 + \left(\frac{|\varepsilon_d|^2}{4\hbar^2}\frac{\Gamma_2^d}{2} + \gamma_{21}\right)^2} - \rho_{22}\frac{\Gamma_2^p}{2} - \rho_{22}\frac{|\varepsilon_d|^2}{4\hbar^2}\frac{\Gamma_3^d\Gamma_2^p}{4}\frac{(q^2-1)\left(\frac{|\varepsilon_d|^2}{4\hbar^2}\frac{\Gamma_2^d+\Gamma_3^d}{2} + \gamma_{32}\right) + 2q\Delta}{\Delta^2 + \left(\frac{|\varepsilon_d|^2}{4\hbar^2}\frac{\Gamma_2^d+\Gamma_3^d}{2} + \gamma_{32}\right)^2}\right]. \quad (20)$$

Similar to Eq. (6), the first term in the above expression describes amplification due to population inversion at the operating transition. The second term, proportional to the population of the emitting excited state and to the rate of absorption of the probe field into the continuum, describes ESA. The third term, which is responsible for ESA suppression, is a consequence of the two-photon coherence σ_{32} built up by the driving and probe fields and due to EIT.

Introducing a dimensionless two-photon detuning

$$x = \frac{\Delta}{\frac{|\varepsilon_d|^2}{4\hbar^2}\frac{\Gamma_2^d+\Gamma_3^d}{2} + \gamma_{32}}$$

we can rewrite Eq. (20) as

$$\mathrm{Im}(P) = -\frac{\varepsilon_p N}{2\hbar}\left[(\rho_{22}-\rho_{11})\frac{|\mu_{21}|^2\left(\frac{|\varepsilon_d|^2}{4\hbar^2}\frac{\Gamma_2^d}{2} + \gamma_{21}\right)}{D^2 + \left(\frac{|\varepsilon_d|^2}{4\hbar^2}\frac{\Gamma_2^d}{2} + \gamma_{21}\right)^2} - \rho_{22}\frac{\Gamma_2^p}{2}\left(\frac{\frac{|\varepsilon_d|^2}{4\hbar^2}\frac{\Gamma_3^d}{2}}{\frac{|\varepsilon_d|^2}{4\hbar^2}\frac{\Gamma_2^d+\Gamma_3^d}{2} + \gamma_{32}}\frac{(x+q)^2}{x^2+1} + \frac{\frac{|\varepsilon_d|^2}{4\hbar^2}\frac{\Gamma_2^d}{2} + \gamma_{32}}{\frac{|\varepsilon_d|^2}{4\hbar^2}\frac{\Gamma_2^d+\Gamma_3^d}{2} + \gamma_{32}}\right)\right]. \quad (21)$$

Here one immediately identifies the first term in large parentheses proportional to $\propto(x+q)^2/(x^2+1)$ as an asymmetric Fano resonance factor [16], responsible for suppression of probe field absorption in the vicinity of a LICS. This absorption is completely canceled at the two-photon detuning $x=-q$. Once it is set to zero, only the second term is left, describing residual excited-state absorption due to decoherence at the Raman transition $3\leftrightarrow 2$. The decoherence rate has two contributions: (1) intrinsic coherence decay rate of the Raman transition γ_{32} and (2) power broadening $(|\varepsilon_d|^2/4\hbar^2)\Gamma_{3,2}^d/2$ due to absorption of the driving field from level 2. If the power broadening is small compared to the intrinsic decay rate (or the driving field intensity is much less than the EIT threshold, which is the same), $(|\varepsilon_d|^2/4\hbar^2)\Gamma_{3,2}^d/2 \ll \gamma_{32}$, then there is no ESA suppression present. But if the intensity greatly exceeds the threshold $[(|\varepsilon_d|^2/4\hbar^2)\Gamma_{3,2}^d/2 \to \infty]$, then the gain factor

$$\mathrm{Im}(P) = -\frac{\varepsilon_p N}{2\hbar}\left[(\rho_{22}-\rho_{11})\frac{|\mu_{21}|^2\left(\frac{|\varepsilon_d|^2}{4\hbar^2}\frac{\Gamma_2^d}{2} + \gamma_{21}\right)}{D^2 + \left(\frac{|\varepsilon_d|^2}{4\hbar^2}\frac{\Gamma_2^d}{2} + \gamma_{21}\right)^2} - \rho_{22}\frac{\Gamma_2^p}{2}\frac{\Gamma_2^d}{\Gamma_2^d+\Gamma_3^d}\right] \quad (22)$$

demonstrates ESA suppression [the second term in Eq. (22)] by a factor of $\Gamma_2^d/(\Gamma_2^d+\Gamma_3^d)$. Note that strong suppression requires $\Gamma_3^d \gg \Gamma_2^d$.

In the most favorable situation when the driving field is not absorbed from state 2, i.e., when $\Gamma_2^d=0$, according to Eq. (21) ESA is suppressed by a factor of $\gamma_{32}/[(|\varepsilon_d|^2/4\hbar^2)\Gamma_3^d/2]$,

which is much less than unity in the EIT regime.

If the driving field is absorbed from state 2, a condition can be derived for lasing to be possible. Neglecting all losses except for ESA of the probe field and assuming the most favorable case $\rho_{11}=0$, one finds that in order to achieve amplification the expression in square brackets in Eq. (22) has to be positive, being equivalent to

$$\sigma_{SE} > \sigma_{ESA}\frac{\Gamma_2^d}{\Gamma_2^d+\Gamma_3^d}\left(1+\frac{|\varepsilon_d|^2}{4\hbar^2}\frac{\Gamma_2^d}{2}/\gamma_{21}\right). \tag{23}$$

The temporal amplification coefficient is then given by the expression

$$\alpha_{\text{gain}} = \frac{cN}{n_p^2}\left(\frac{\sigma_{SE}}{1+\frac{|\varepsilon_d|^2}{4\hbar^2}\frac{\Gamma_2^d}{2}/\gamma_{21}} - \sigma_{ESA}\frac{\Gamma_2^d}{\Gamma_2^d+\Gamma_3^d}\right). \tag{24}$$

Even if it is positive, there has to be enough time for generation to develop before the upper operating state is depleted by ionization due to ESA of the driving field. In other words, in order for laser oscillation to build up the gain has to exceed the rate at which population is pumped out of state 2 into the continuum:

$$\alpha_{\text{gain}} > \frac{|\varepsilon_d|^2}{4\hbar^2}\frac{\Gamma_2^d}{2}.$$

It yields the following requirement for the inversion density:

$$N > \frac{n_p^2\frac{|\varepsilon_d|^2}{2\hbar^2}\frac{\Gamma_2^d}{2}}{c\left(\sigma_{SE}/\left(1+\frac{|\varepsilon_d|^2}{4\hbar^2}\frac{\Gamma_2^d}{2}/\gamma_{21}\right)-\sigma_{ESA}\frac{\Gamma_2^d}{a_2^d+\Gamma_3^d}\right)}. \tag{25}$$

This requirement is a consequence of the fact that the temporal gain is proportional to the density of inverted atoms while the photoionization rate is independent of density and is determined only by the driving field intensity and photoionization efficiency. Thus, the higher the density the more likely laser generation is to develop before the inversion is pumped out by the driving field.

III. DISCUSSION

In the present section we discuss how the proposed method of ESA reduction can be applied to realize uv lasing in rare-earth-ion-doped crystals. Typically in these materials ESA transitions terminate in the CB of a host, so we mostly focus on this situation.

Let us turn to estimates for required driving field intensities for typical parameters of rare earths, assuming that the driving field does not cause photoionization from level 2.

In the previous section it was shown that ESA is suppressed if the driving field intensity exceeds a threshold value, necessary for EIT to be established:

$$\frac{|\varepsilon_d|^2}{4\hbar^2}\frac{\Gamma_3^d}{2} \gg \gamma_{32}. \tag{26}$$

The ionization rate Γ_3^d for the driving field from level 3 can be expressed in terms of the ionization cross section as $\sigma_3^d = 2\pi\omega_d\Gamma_3^d/\hbar c$, while the field amplitude can be written as $|\varepsilon_d|^2 = 8\pi I^d/c$ in terms of intensity. The condition (26) can then be rewritten as

$$\frac{I^d\sigma_3^d\lambda_d}{4\pi\hbar c} \gg \gamma_{32},$$

leading to the threshold intensity

$$I^d \gg I_{th}^d = \gamma_{32}\frac{4\pi\hbar c}{\sigma_3^d\lambda_d}. \tag{27}$$

As follows from Eq. (27), the threshold intensity is proportional to the Raman transition coherence decay rate γ_{32} (here γ_{32} has actually to be replaced by an inhomogeneous width W_{32}^{inh}) and inversely proportional to the driving field wavelength and ionization cross section from level 3. Thus, to achieve a lower threshold intensity, a Raman transition width as narrow as possible, a driving field wavelength as long as possible, and an ionization cross section from state 3 into the CB as large as possible are required.

We consider two different configurations when level 2 is either of $4f^n$ or $4f^{n-1}5d$ type. In the first case the operating laser transition $2\leftrightarrow 1$ is intraconfigurational $4f^n\leftrightarrow 4f^n$, while in the latter case it is of interconfigurational $4f^{n-1}5d\leftrightarrow 4f^n$ type. The auxiliary level 3 should be of the same type as the upper operating level 2, so that the driving field can couple it to the same continuum to which level 2 is coupled by the probe field. In other words, this is the requirement for existence of a Λ system which involves driving and probe fields, two discrete states 2 and 3, and the same continuum. It means that the Raman transition $2\leftrightarrow 3$ should be of intraconfigurational $4f^n\leftrightarrow 4f^n$ or $4f^{n-1}5d\leftrightarrow 4f^{n-1}5d$ type.

The widths of $4f^n\leftrightarrow 4f^n$ transitions can vary from tens of megahertz [19,20] in the best case to hundreds of gigahertz in the worst case. However, in good quality crystals most linewidths of such transitions lie in the range 1–10 GHz. Typical photoionization cross sections from $4f^n$ states are $\sigma_{ESA}\sim 10^{-18}$ cm^2. Assuming the wavelength of the driving field to lie in the range $\lambda_d\sim 0.3$–1 μm, we obtain the following estimate for the threshold intensity:

$$I_{th}^d \sim (1-100)\frac{\text{GW}}{\text{cm}^2}.$$

The situation is more complicated if the emitting state 2 is of $4f^{n-1}5d$ type. The driving field intensity estimate depends on how narrow the transition $2\leftrightarrow 3$ between the two $4f^{n-1}5d$ states can be made. There is no direct experimental data on these transition widths, so for an estimate we make the rather reasonable assumption that this width is of the same order as a typical linewidth of a $4f^n\leftrightarrow 4f^{n-1}5d$ transition. We should stress that this is the upper limit for the $4f^{n-1}5d\leftrightarrow 4f^{n-1}5d$ linewidth; it actually might be narrower. It is known that at room temperature $4f^{n-1}5d\rightarrow 4f^n$ emission and absorption form wide bands with a total bandwidth of several tens or even hundreds of nanometers. However, this width originates from phonon sidebands of absorption/emission spectra. The lifetime of phonon states is very short (typically, in the picosecond range) compared to the metastable laser state lifetime; thus, the states with excited phonons cannot give rise to

ESA. Where ESA truly originates is in the pure electronic excited state of a dopant. The widths of these states can be very narrow compared to the total bandwidth of a transition. This fact is confirmed by low-temperature absorption and fluorescence measurements in crystals doped with rare earths, where pure electronic transition [so called zero-phonon line (ZPL)] widths as narrow as 1 cm^{-1} and even smaller were observed. For example, in cerium-doped CaF_2 crystals the width of the ZPL was found to be 0.64 cm^{-1} at low temperature (6 K) [21]. A ZPL of the same width (1.6 cm^{-1}) was observed for the $4f^{13}5d \leftrightarrow 4f^{14}$ transition in Yb^{2+} doped into MgF_2 [8]. Generally, at low temperatures linewidths of the order of 10–100 GHz can be obtained. Taking into account the fact that photoionization cross sections from $4f^{n-1}5d$ states in lanthanides are $\sigma_{ESA} \sim 10^{-17}-10^{-18}$ cm^2 and assuming the same driving field wavelength range as in the above estimate, we arrive at approximately the same value for the driving field intensity as in the case of an intraconfigurational operating transition:

$$I_{th}^{d} \sim (10-100)\frac{\mathrm{GW}}{\mathrm{cm}^2}.$$

However, data about ZPL widths of interconfigurational transitions are scarce, so in each particular case the possibility of reducing ESA from a $4f^{n-1}5d$ state should be carefully studied experimentally.

Such intensities are achievable in a pulsed regime. For example, for a 1 ns pulse, focused to a spot of 100 μm diameter, required energies of the driving laser pulse are 0.1–10 mJ. It is necessary though that this intensity be smaller than the damage threshold intensity of a crystal.

The distinction between inter- and intraconfigurational operating transitions is crucial with respect to potential laser tunability. Typically, for $4f^n \leftrightarrow 4f^n$ transitions phonon sidebands in both emission and absorption are very weak, so that laser action can be realized only at a fixed frequency. Tunability in this case is restricted by the width of the electronic transition and cannot go beyond ~10 GHz. On the other hand, for $4f^{n-1}5d \leftrightarrow 4f^n$ transitions phonon-assisted emission, redshifted with respect to the ZPL, can be very broad (tens of nanometers). By applying a driving field of a certain frequency, one can reduce ESA losses for some particular wavelength within the phonon sideband of $4f^{n-1}5d \leftrightarrow 4f^n$ fluorescence. Thus, the desired laser wavelength can be chosen by tuning the frequency of the driving field.

As an example we consider a Pr^{3+}:$LiLuF_4$ crystal, which is a promising material for a uv laser [4,22], since $4f5d$ states of the Pr^{3+} ion can be efficiently populated by two-step up-conversion pumping via intermediate metastable $4f^2$ levels. This pumping scheme helps to avoid color center formation due to ESA of uv pump photons into the CB. There was an attempt to achieve amplification on the $4f5d(1) \rightarrow {}^3H_4$ transition at $\lambda = 255$ nm [23] under such up-conversion pumping, but instead of gain 65% absorption of the probe beam was detected. As the authors point out, it was not successful due to ESA of probe photons from the $4f5d(1)$ emitting state into the CB. This problem can be overcome by the method proposed in the present paper; namely, an additional

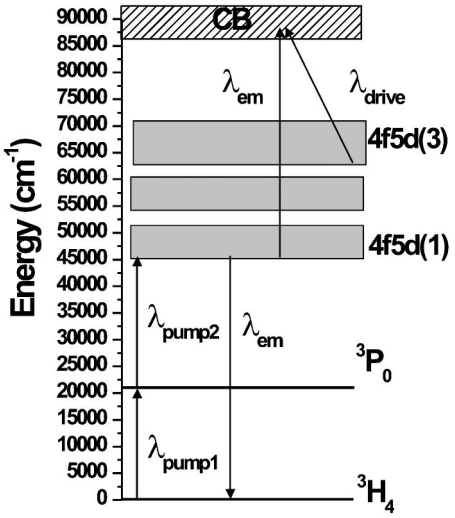

FIG. 4. Energy level scheme of Pr^{3+} ion in $LiLuF_4$.

driving laser beam can be applied at another $4f5d \rightarrow$ CB transition in the way shown in Fig. 4. Room temperature emission from the lowest $4f5d(1)$ state occurs between 220 and 280 nm (35710–45450 cm^{-1}), and transition to the ${}^3H_4$ level has a wavelength of 222 nm [24]. The emitted photons are therefore absorbed in the CB at a wave number range of ~82 000–92 000 cm^{-1}. The third $4f5d(3)$ band in the excitation spectrum is at ~62 000 cm^{-1}(161 nm) and the driving field can be applied to the $4f5d(3) \rightarrow$ CB transition. The required wavelength of the driving field is in the range 500–330 nm, which corresponds to the difference in energy 20 000–30 000 cm^{-1} between $4f5d(3)$ and the terminal state of ESA. If a two-step pumping scheme is used via the ${}^3P_0$ intermediate level, the second step pump field can simultaneously serve as the driving field, since pumping into $4f5d(1)$ from ${}^3P_0$ requires wavelengths in the range 330–400 nm. By tuning the pump (and, simultaneously, driving) field, uv gain in the wavelength range of 220–240 nm can be expected. A driving field of the wavelength 330–400 nm will not be absorbed from the ground ${}^3H_4$ state and it will be only weakly absorbed from the emitting $4f5d(1)$ state into the high-energy edge of the $4f5d(3)$ band at 70 000–75 000 cm^{-1} due to the parity-forbidden character of $5d \leftrightarrow 5d$ transitions. The intensity of the drive field required to establish EIT and suppress ESA, given by Eq. (27), cannot be estimated because the decay rate of $4f5d(1) \leftrightarrow 4f5d(3)$ coherence is not known. Zero-phonon lines were observed in Pr^{3+}:$LiYF_4$ at low temperature (8 K) only for the first $4f5d(1)$ band [25], so it is not clear what is the rate of coherence decay between the two $4f5d$ states, connected by driving and probe fields.

In Pr^{3+}:$LiYF_4$ it was found that the ESA cross section from the first $4f5d(1)$ band into the CB is comparable with the emission cross section [$\sigma_{EM} = (2.0 \pm 0.2) \times 10^{-18}$ cm^2, $\sigma_{ESA} = (2.6 \pm 0.5) \times 10^{-18}$ cm^2 at room temperature] [9], so ESA needs to be suppressed only by a small amount in order to achieve positive gain.

ESA to the CB becomes important when the frequency of generated light is larger than $\omega_{BG}/2$, where ω_{BG} is the fre-

quency of the onset of absorption from the ground state of an ion into the CB. It is certainly feasible to make the generated frequency as close as possible to ω_{BG}. However, it requires shorter wavelengths of the driving field. The requirement that the driving field is not absorbed from the emitting level into the CB means that $\omega_d < \omega_{BG} - \omega_{EM}$. On the other hand, the driving field frequency obviously satisfies the condition $\omega_d > 2\omega_{EM} - \omega_{BG}$, which is the consequence of the fact that state 3 lies in the band gap of the crystal. These two conditions set a limit on the generated wavelength of a solid-state laser with suppressed ESA:

$$\omega_{EM} < 2\omega_{BG}/3. \tag{28}$$

In wide band gap fluoride crystals, such as $LiYF_4$, $LiLuF_4$, YF_3, and LaF_3, the energy difference between the ground state of a dopant ion and the CB does not exceed $\sim 80\ 000\ cm^{-1}$; then, according to Eq. (28), the generated field wavelength is limited from below by $\lambda_{EM} > 190$ nm.

Apart from the discussion on rare-earth-ion-doped materials as potential candidates for solid-state uv lasing, we would like to mention that the same technique of ESA reduction can be implemented to realize infrared lasing in crystals doped with transition metal ions. Of course, many laser crystals for this range already exist, but far more crystals do not lase due to ESA into either a charge transfer band or into a higher-lying electronic state. Examples of crystals in which the proposed technique can be helpful to achieve lasing are $V^{3+}:LiAlO_2$, $LiGaO_2$ (luminescence at 1400–1800 nm) [26], $Cr^{4+}:LiAlO_2$ $LiGaO_2$(luminescence at 1200–1600 nm) [27], $Ni^{2+}:MgAl_2O_4$ (luminescence at 1100–1300 nm) [28], and some others. For these materials the driving field wavelength lies in the visible or near infrared range.

IV. CONCLUSION

In conclusion we theoretically demonstrate that excited-state absorption, which prevents the realization of uv or vuv lasers in rare-earth- or transition-metal-ion-doped crystals, can be greatly reduced by applying an additional driving laser field. The approach is based on the effect of electromagnetically induced transparency. Estimates for typical parameters of laser crystals show that requirements for the driving field are experimentally doable and reasonable. Hence, the suggested method of ESA suppression seems to be practical and promising for realization of new solid-state uv lasers. An additional advantage of the proposed technique is that it allows one to tune the laser wavelength by tuning the driving field wavelength due to selective reduction of the lasing threshold in a narrow spectral region in the vicinity of a two-photon resonance with the driving field.

ACKNOWLEDGMENTS

The authors are grateful to Yuri Rostovtsev for many interesting and stimulating discussions. This work was supported by NSF, ONR, and the Texas Advanced Research Program.

[1] S. Kück, Appl. Phys. B: Lasers Opt. **72**, 515 (2001).
[2] D. J. Ehrlich, P. F. Moulton, and R. M. Osgood, Opt. Lett. **4**, 184 (1979); D. J. Ehrlich, P. F. Moulton, and R. M. Osgood, *ibid.* **5**, 339 (1980); M. A. Dubinskii, V. V. Semashko, A. K. Naumov, R. Yu. Abdulsabirov, and S. L. Korableva, Laser Phys. **3**, 216 (1993); C. D. Marshall, J. A. Speth, S. A. Payne, W. F. Krupke, G. J. Quarles, V. Castillo, and B. H. T. Chai, J. Opt. Soc. Am. B **11**, 2054 (1994).
[3] R. W. Waynant, Appl. Phys. B: Photophys. Laser Chem. **28**, 205 (1982); R. W. Waynant and P. H. Klein, Appl. Phys. Lett. **46**, 14 (1985).
[4] M. F. Joubert and R. Moncorge, Opt. Mater. (Amsterdam, Neth.) **22**, 95 (2003).
[5] S. Nicolas *et al.*, J. Phys.: Condens. Matter **11**, 7937 (1999).
[6] Y. M. Cheung and S. K. Gayen, Phys. Rev. B **49**, 14827 (1994).
[7] D. S. Hamilton *et al.*, Phys. Rev. B **39**, 8807 (1989).
[8] S. Lizzo, A. Meijerink, G. J. Dirksen, and G. Blasse, J. Lumin. **63**, 223 (1995).
[9] J. K. Lawson and S. A. Payne, Opt. Mater. (Amsterdam, Neth.) **2**, 225 (1993).
[10] S. A. Payne, C. D. Marshall, A. J. Bayramian, and J. K. Lawson, Proc. SPIE **3176**, 68 (1997).
[11] J. S. Cashmore, S. M. Hooker, and C. E. Webb, Appl. Phys. B: Lasers Opt. **64**, 293 (1997).
[12] S. E. Harris, Phys. Today **50**(7), 36 (1997); E. Arimondo, in *Progress in Optics XXXV*, edited by E. Wolf (Elsevier Science, Amsterdam, 1996), pp. 257–354; O. A. Kocharovskaya and Ya. I. Khanin, Zh. Eksp. Teor. Fiz. **90**, 1610 (1986) [Sov. Phys. JETP **63**, 945 (1986)] ; M. O. Scully and M. S. Zubairy, *Quantum Optics* (Cambridge University Press, Cambridge, U.K., 1997).
[13] R. C. Alig, Z. J. Kiss, J. P. Brown, and D. S. McClure, Phys. Rev. **186**, 276 (1969).
[14] G. S. Agarwal and W. Harshawardhan, Phys. Rev. Lett. **77**, 1039 (1996); M. Yan, E. G. Rickey, and Y. Zhu, Phys. Rev. A **64**, 043807 (2001).
[15] E. Kuznetsova, O. Kocharovskaya, P. Hemmer, and M. O. Scully, Phys. Rev. A **66**, 063802 (2002).
[16] U. Fano, Phys. Rev. **124**, 1866 (1961).
[17] P. L. Knight, M. A. Lauder, and B. J. Dalton, Phys. Rep. **190**, 1 (1990).
[18] K. Böhmer *et al.*, Phys. Rev. A **66**, 013406 (2002).
[19] R. M. Macfarlane, A. Cassanho, and R. S. Meltzer, Phys. Rev. Lett. **69**, 542 (1992).
[20] R. M. Macfarlane, R. S. Meltzer, and B. Z. Malkin, Phys. Rev. B **58**, 5692 (1998).
[21] S. K. Gayen, D. S. Hamilton, and R. H. Bartram, Phys. Rev. B **34**, 7517 (1986).
[22] E. Sarantopoulou *et al.*, Opt. Lett. **19**, 499 (1994).
[23] S. Nicolas *et al.*, Opt. Mater. (Amsterdam, Neth.) **22**, 139 (2003).

[24] S. Nicolas *et al.*, Opt. Mater. (Amsterdam, Neth.) **16**, 233 (2001).
[25] M. Laroche *et al.*, J. Opt. Soc. Am. B **17**, 1291 (2000).
[26] S. Kück and P. Jander, Opt. Mater. (Amsterdam, Neth.) **13**, 299 (1999).
[27] S. Kück and S. Hartung, Chem. Phys. **240**, 387 (1999).
[28] N. V. Kuleshov *et al.*, J. Lumin. **71**, 265 (1997).